Photochemical transformation of ibuprofen into harmful 4-isobutylacetophenone: Pathways, kinetics, and significance for surface waters

(Article begins on next page)

29 May 2024

Photochemical transformation of ibuprofen into harmful 4-isobutylacetophenone: Pathways, kinetics, and significance for surface waters

Giulia Ruggeri,[a] Giovanni Ghigo,[a] Valter Maurino,[a] Claudio Minero,[a] and Davide Vione [a,b]∗

[a] *Università degli Studi di Torino, Dipartimento di Chimica, Via Pietro Giuria 5-7, 10125 Torino, Italy.*

[b] *Centro Interdipartimentale NatRisk, Università di Torino, Via L. Da Vinci 44, 10095 Grugliasco (TO), Italy.*

∗ Corresponding author. Phone +39-011-6705296; Fax +39-011-6705242; E-mail: davide.vione@unito.it

ABSTRACT

The harmful compound 4-isobutylacetophenone (IBAP) can be formed photochemically from the anti-inflammatory drug ibuprofen (IBP), upon direct photolysis (yield 25±7%, μ±σ), reaction with $^\bullet$OH (yield 2.3±0.1%) and reaction with triplet states of chromophoric dissolved organic matter, ^{3}CDOM* (yield 31±4%). In the latter case, anthraquinone-2-sulphonate was used as CDOM proxy. The three processes would account for most of the photochemical transformation of IBP and IBAP in surface waters. IBAP formation from IBP involves the propanoic acid chain, which is more reactive than the aromatic ring as shown by quantum mechanical calculations. IBAP is expected to undergo slightly faster photochemical transformation than IBP in surface waters, with a modelled pseudo-first order rate constant that is higher by 1.5-1.9 times compared to IBP. Due to fairly high formation yields and depending on IBP emission scenarios, photochemical modelling suggests that IBAP could reach concentration values up to ~15% of IBP in surface waters, thus being a potentially important transformation intermediate. This issue prompts for the need of field studies that provide information on IBAP environmental occurrence, which is virtually unknown at the present moment.

Keywords: surface-water photochemistry; photosensitised transformation; transformation by-products and intermediates; non-steroidal anti-inflammatory drugs; radical reactions.

1. INTRODUCTION

Ibuprofen (2-[4-(2-methylpropyl)phenyl]propanoic acid, hereafter IBP) is a non-steroidal anti-inflammatory drug (NSAID) that is widely used nowadays as the active principle of many "over the counter" pharmaceutical products, including analgesics and antipyretics (Kanabar et al., 2007). The widespread use of IBP is the main reason for its common detection in both wastewater and surface water, at concentration levels of ng L^{-1} or even µg L^{-1} (Buser et al., 1999; Andreozzi et al., 2003; Tixier et al., 2003; Carballa et al., 2004; Castiglioni et al., 2006). This compound together with other NSAIDs is also a cause of concern for drinking water, where residues have been detected (at ng L^{-1} levels in the case of IBP; Mompelat et al., 2009).

Bio- and photodegradation are the main transformation routes of IBP in surface waters (Packer et al., 2003; Lin et al., 2006; Peuravuori and Pihlaja, 2009; Kunkel and Radke, 2011; Jacobs et al., 2011). As far as IBP phototransformation is concerned, there is massive evidence that it can be carried out efficiently in technological systems under photocatalytic conditions (Molinari et al., 2006; Mendez-Arriaga et al., 2008; Achilleos et al., 2010; Miranda-Garcia et al., 2011; Choina et al., 2013). In the case of surface waters, it has been shown recently that the main pathways involved in IBP transformation would be photolysis, reaction with $^{\bullet}$OH and with the triplet states of chromophoric dissolved organic matter (^{3}CDOM*) (Vione et al., 2011). Direct photolysis in surface waters takes place upon sunlight absorption by a dissolved substrate, which is then transformed *via* bond breaking, isomerisation or ionisation. The radicals $^{\bullet}$OH are mainly produced upon irradiation of nitrite, nitrate and CDOM and they are mostly scavenged by dissolved organic matter (DOM, both chromophoric and not). Formation of ^{3}CDOM* involves radiation absorption by CDOM followed by inter-system crossing. Important sinks of ^{3}CDOM* are thermal deactivation and reaction with dissolved O_2 to produce $^{1}O_2$ (Canonica and Freibirghaus, 2001; Boreen et al., 2003; Richard et al., 2007; Al Housari et al., 2010).

Among IBP transformation intermediates, 4-isobutylacetophenone (IBAP) is formed by several pathways and causes concern because of its adverse effects on connective tissue cells, red blood cells and the central nervous system (Castell et al., 1987; Miranda et al., 1991; Volonte et al., 2005; Cory et al., 2010; Sabri et al., 2012). Interestingly, IBAP formation has been detected *via* all the three main pathways of IBP photodegradation, namely direct photolysis and reactions with $^{\bullet}$OH and ^{3}CDOM* (Vione et al., 2011). Unfortunately, very few data are reported on the environmental occurrence of IBAP (Zorita et al., 2007), and virtually no data are available on its persistence. At the present state of knowledge, it is extremely difficult to state if and to what extent IBAP is an IBP transformation intermediate of environmental concern.

This work has the goal of assessing the significance of IBP photochemical transformation into IBAP, thereby providing the first assessment of IBAP environmental importance. To this purpose we studied: *(i)* the reaction pathway, to explain why the detected IBP photo-intermediates are produced by transformation of lateral chains rather than the aromatic ring; *(ii)* the formation kinetics

3

and yields of IBAP from IBP, *via* the main phototransformation processes that involve IBP in surface waters (direct photolysis and reaction with $^\bullet OH$ and $^3CDOM^*$), and *(iii)* the transformation kinetics of IBAP *via* the photochemical processes that usually prevail in surface waters: direct photolysis and reaction with $^\bullet OH$, $^3CDOM^*$, $^1O_2$ and $CO_3^{-\bullet}$ (Huang and Mabury, 2000; Boreen et al., 2003; Canonica et al., 2005). These data, combined with a photochemical model (Sur et al., 2012; De Laurentiis et al., 2012), allow an assessment of the photogeneration of IBAP from IBP, together with the identification of environmental conditions where the process could be most important. In this way, it is possible to get some insight into the otherwise unknown formation and reactivity of IBAP in surface waters.

2. MATERIALS AND METHODS

2.1. Reagents. Ibuprofen (IBP, purity grade 98%), anthraquinone-2-sulphonic acid, sodium salt (AQ2S, 97%), furfuryl alcohol (98%), $NaNO_3$ (>99%), $NaHCO_3$ (98%), $HClO_4$ (70%) and H_3PO_4 (85%) were purchased from Aldrich, NaOH (99%), methanol and 2-propanol (both gradient grade) from Carlo Erba, Rose Bengal (RB) and 4-isobutylacetophenone (IBAP, 97%) from Alfa Aesar.

2.2. Irradiation experiments. Solutions to be irradiated (5 mL) were placed inside cylindrical Pyrex glass cells (4.0 cm diameter, 2.3 cm height, 295 nm cut-off wavelength), closed with a lateral screw cap. Cells were magnetically stirred during irradiation, which occurred mainly from the top. The choice of lamps for irradiation depended on the experiments to be carried out, and on the need to excite some photoactive compounds as selectively as possible. In particular, a Philips TL 20W/01 RS UVB lamp was used for experiments of direct irradiation of IBP and IBAP, for exciting H_2O_2 to produce $^\bullet OH$, and for irradiating $NaNO_3$ + $NaHCO_3$ to test reactivity between IBAP and $CO_3^{-\bullet}$. The lamp has emission maximum at 313 nm and 13.0±0.6 W m^{-2} UV irradiance (290-400 nm), measured with a power meter by CO.FO.ME.GRA. (Milan, Italy). The incident photon flux in solution was P_o = (8.53±0.39)×10^{-6} Einstein L^{-1} s^{-1}, actinometrically determined with the ferrioxalate method (Kuhn et al., 2004). Irradiation of anthraquinone-2-sulphonate (AQ2S) as CDOM proxy to assess $^3CDOM^*$ reactivity was carried out under a Philips TLK 05 UVA lamp, with emission maximum at 365 nm, 31.4±1.0 W m^{-2} UV irradiance, and P_o = (2.38±0.11)×10^{-5} Einstein L^{-1} s^{-1} incident photon flux. Irradiation of Rose Bengal as $^1O_2$ source was carried out under a Philips TL D 18W/16 yellow lamp. The lamp had emission maximum at 545 nm and 11±1 W m^{-2} irradiance in the visible. Lamp spectra were measured with an Ocean Optics USB 2000 CCD spectrophotometer and were normalised to actinometry data. These spectra are reported in Figure 1, together with absorption spectra of photoactive species, measured with a Varian Cary 100 Scan UV-Vis spectrophotometer.

AQ2S was chosen as CDOM proxy because quinones are important photoactive compounds in CDOM (Cory and McKnight, 2005). Furthermore, AQ2S does not yield (or yields to a low or

negligible extent) interfering species such as $^1O_2$ or $^\bullet OH$ upon irradiation. The reason is that $^3AQ2S^*$ undergoes very fast reaction with H_2O to form water adducts, which evolve into ground-state AQ2S or into hydroxyderivatives. The fast reaction with the solvent prevents reaction between $^3AQ2S^*$ and O_2 to be significant (Loeff et al., 1983; Maddigapu et al., 2010). The lack of formation of $^\bullet OH$ and $^1O_2$ is very important in this context. Indeed, while one can try to block reactivity of $^1O_2$ and $^\bullet OH$ produced by triplet sensitisers (different from AQ2S) by addition of scavengers, it is not possible to exclude reactions of the triplet states themselves with the scavengers (Maddigapu et al., 2010; Bedini et al., 2012). Such reactions would bias the kinetic data. Therefore, although $^3AQ2S^*$ may be more reactive than average triplet states toward organic compounds (which has been taken into account in the discussion, *vide infra*) (Maddigapu et al., 2010), because an ideal CDOM proxy is presently unavailable, we considered AQ2S as the most suitable compound for our experimental approach. Another aspect in favour of AQ2S is that its well-known photochemistry allows the measurement of triplet-state reactivity by steady irradiation experiments alone. The initial AQ2S concentration (0.1 mM) was chosen to avoid additional complications from reaction between $^3AQ2S^*$ and ground-state AQ2S (Bedini et al., 2012).

2.3. Analytical determinations. The time evolution of IBP and IBAP was monitored by liquid chromatography, using a VWR-Hitachi LaChrom Elite chromatograph equipped with L-2200 autosampler (injection volume 60 µL), L-2130 quaternary pump for low-pressure gradients, L-2300 column oven, and L-2455 photodiode array detector. The column was a VWR LiChroCART 125-4 Cartridge, packed with LiChrospher 100 RP-18 (125mm×4 mm×5µm). The eluent (1.0 mL min^{-1} flow rate) was a 55:45 mixture of methanol:aqueous H_3PO_4 (pH 2.8) and retention times were 23.0 min (IBAP) and 25.8 min (IBP), with 0.9 min column dead time. Detection wavelengths for IBP and IBAP were 220 nm and 256 nm, respectively. Furfuryl alcohol, used to quantify $^1O_2$ photogeneration by Rose Bengal (Sur et al., 2012; De Laurentiis et al., 2012), was eluted with a 15:85 mixture of methanol:aqueous H_3PO_4 (1.0 mL min^{-1}) and detected at 230 nm. Its retention time was 4.50 min.

The solution pH was adjusted with $HClO_4$ or NaOH and measured with a combined glass electrode, connected to a Metrohm 713 pH meter. Changes of pH during irradiation were monitored and they were included within 0.3 pH units.

2.4. Kinetic data treatment. The time evolution of IBP was fitted with pseudo-first order equations $c_t = c_o \times e^{-k_{IBP} \times t}$, where c_t is IBP concentration at the time t, c_o its initial concentration, and k_{IBP} the pseudo first-order transformation rate constant. IBAP time evolution was fitted with $c'_t = (k_{IBAP})' c_o (k_{IBAP} - k_{IBP})^{-1} (e^{-k_{IBP} \times t} - e^{-k_{IBAP} \times t})$, where c_o and k_{IBP} are as above, c'_t is the concentration of IBAP at the time t, $(k_{IBAP})'$ is the rate constant of IBAP formation from IBP, and k_{IBAP} is the rate constant of IBAP transformation. The initial rates of IBP transformation and IBAP formation are $r_{IBP} = k_{IBP} \times c_o$ and $r'_{IBAP} = (k_{IBAP})' \times c_o$, respectively. The errors on the rates (±σ) were

5

derived from the scattering of experimental data around fit curves. Reproducibility of repeated runs was ~15%. All data fits were carried out with the Fig.P software package (Biosoft, UK).

2.5. Photochemical model. The environmental significance of reactivity data obtained in the laboratory was assessed by means of a photochemical model that links water chemistry and substrate photoreactivity (Vione et al., 2011; Maddigapu et al., 2011; Sur et al., 2012). Half-life times and first-order reaction rate constants of compounds dissolved in well-mixed surface waters are predicted using: *(i)* sunlight irradiance and spectrum; *(ii)* substrate reactivity data (photolysis quantum yield and reaction rate constants with $^\bullet OH$, $CO_3^{-\bullet}$, $^1O_2$ and $^3CDOM^*$); *(iii)* water parameters of photochemical significance (depth, concentrations of nitrate, nitrite, bicarbonate and carbonate, dissolved organic carbon (DOC)). If not available, water absorption spectrum is modelled from the DOC value. Competition of photoactive compounds for sunlight irradiance (including IBP and IBAP) is taken into account at each relevant wavelength in a Lambert-Beer approach (Sur et al., 2012). Half-life times and reaction rate constants are given in units of SSD and SSD^{-1}, respectively, where SSD (summer sunny day) is equivalent to fair-weather 15 July at 45°N latitude and takes the day-night cycle into account. The model has predicted the phototransformation kinetics of several substrates (including IBP) in fresh- and brackish-water environments, in good agreement with available field data (Vione et al., 2011; Maddigapu et al., 2011; Sur et al., 2012; De Laurentiis et al., 2012). The model can also predict the formation kinetics of intermediates, based on their formation yields from the substrate *via* the relevant photochemical pathways (De Laurentiis et al., 2012). We have recently derived a software application from the model (APEX: Aqueous Photochemistry of Environmentally-occurring Xenobiotics), which is available for free download at *http://chimica.campusnet.unito.it/do/didattica.pl/Quest?corso=7a3d* (including the User's Guide that contains a comprehensive account of model equations). APEX was extensively used in the modelling sections of this manuscript.

3. RESULTS AND DISCUSSION

3.1. Photoinduced formation of IBAP from IBP (irradiation experiments)

The only important photochemical processes that can account for IBP transformation (and IBAP formation) in surface waters are direct photolysis and reactions with $^\bullet OH$ and $^3CDOM^*$ (Vione et al., 2011). Therefore, the formation yields of IBAP from IBP were determined under the corresponding conditions as the ratios between IBAP initial formation rates and IBP initial transformation rates, $\eta_{Phot}^{IBP \to IBAP} = r_{IBAP} \times (r_{IBP})^{-1}$.

3.1.1. IBP direct photolysis

Figure 2a reports the time trends of 0.10 mM IBP and IBAP in neutral solution upon UVB irradiation, which was chosen because IBP absorbs sunlight in the UVB region. The error bars represent the standard deviation of runs carried out in duplicate. Under this experimental setup, the half-life time of IBP was around 25 h. The yield of IBAP from IBP upon direct photolysis was determined as the ratio between IBAP initial formation rate and IBP initial transformation rate, $\eta_{Phot}^{IBP \to IBAP} = r'_{IBAP} \times (r_{IBP})^{-1} = 0.25 \pm 0.07$. The value of $\eta_{Phot}^{IBP \to IBAP}$ showed a significant pH trend: in the pH interval 2-3 it was about one-third than for pH 7.2, suggesting that the direct photolysis of anionic IBP produces IBAP more effectively compared to protonated IBP ($pK_a = 4.4$; Martell et al., 1997). The yield value increased at pH 4 and 5, and at pH 6 it was only ~10% lower than at pH 7.2, which is within experimental uncertainty. Therefore, the pH trend of $\eta_{Phot}^{IBP \to IBAP}$ would be mostly accounted for by the acid-base equilibrium between protonated and anionic IBP.

3.1.2. Reaction between IBP and •OH

The reaction with •OH is by a large far the simplest one to be studied by computational methods, while the others are much more difficult to be tackled. For this reason, although •OH was not the process yielding IBAP in highest yield (*vide infra*), a number of primary reaction pathways with •OH were computationally investigated: hydrogen extractions (Scheme 1a) from the tertiary carbon of the propanoic acid chain (xO, which is the pathway that would likely produce IBAP), from the secondary carbon of the isobutyl chain (xC), or from the tertiary carbon of the isobutyl chain (xP). It was also studied the •OH addition to the aromatic ring (Scheme 1b, in four non-equivalent positions, Add1-4), which would finally yield the corresponding phenols. These are all typical reactions of the hydroxyl radical with insaturated organic compounds. A consistency check for calculations was carried out, by assessing the second-order reaction rate constant between anionic IBP and •OH by means of the Eyring equation (Frisch et al., 2009). Calculations yielded $k_{IBP,•OH} = 3.6 \times 10^9$ M^{-1} s^{-1}, in reasonable agreement with the experimental value of $1.0 \cdot 10^{10}$ M^{-1} s^{-1} (Vione et al., 2011). Details of the calculations are reported as SM and only a brief summary is given here.

Calculation results showed that H extractions are kinetically favoured over ring additions by 2-3 kcal mol^{-1}. This is due to the destruction of the aromaticity in the adducts and to the unfavourable entropic effect, and it explains the lack of detection of ring-hydroxylated IBP intermediates that could arise from Add1-4. In contrast, detected intermediates of IBP + •OH would mainly arise from the xO pathway. Among such intermediates we can also include products found by Jacobs et al. (2011), which were hydroxylated in the lateral chains, while the phenols found by the same authors should come out from a different degradation channel.

Figure 2b reports the time trends of 0.11 mM IBP and of IBAP, upon UVB irradiation of 1.0 mM H$_2$O$_2$ (photochemical •OH source; Buxton et al., 1988) in neutral solution. Note that IBAP

concentration in the figure is multiplied by 10, so that it could be plotted against the same Y-axis scale as IBP. It was found $r'_{IBAP} (r_{IBP})^{-1} = 0.032 \pm 0.009$, implying that the IBAP yield under such conditions was almost one order of magnitude lower compared to the direct photolysis. Because H_2O_2 and IBP both absorb UVB radiation, IBP could undergo direct photolysis to some extent in the presence of H_2O_2, which could contribute to IBAP formation.

The molar absorption coefficients of H_2O_2 and IBP at 313 nm (the wavelength of lamp maximum emission) were measured as $\varepsilon_{H_2O_2} = 0.20$ M^{-1} cm^{-1} and $\varepsilon_{IBP} = 4.6$ M^{-1} cm^{-1}. The optical path length in solution was $b = 0.4$ cm. Therefore, the absorbance values of 1.0 mM H_2O_2 and 0.11 mM IBP were low enough to ensure that the two species absorb radiation independently. This issue makes it easier to assess the contribution of direct photolysis to IBP transformation and IBAP formation, by comparing data reported in Figure 2a and Figure 2b. In the case of IBP + H_2O_2, one obtains that direct photolysis would account for 4.3±0.9% of IBP transformation and for 30±5% of IBAP formation, the remainder being accounted for by $^\bullet$OH. By correcting r'_{IBAP} and r_{IBP} for the direct photolysis contribution, one obtains $\eta^{IBP \to IBAP}_{\bullet OH} = 0.023 \pm 0.010$.

The IBAP yield from IBP upon H_2O_2 irradiation decreased with increasing pH: it was around 0.16 at pH 2, 0.08 at pH 3, and stabilised at ~0.03 above pH 5. The relative role of direct photolysis is expected to be lower under acidic conditions, because $\eta^{IBP \to IBAP}_{Phot}$ decreased with decreasing pH. The different yield values at pH 2 and 3 suggest that the acid-base equilibrium between protonated and anionic IBP would not account for the whole pH effect. The latter may also be due to further transformation processes following the primary reaction step (which is most likely the xO pathway as previously discussed).

Note that we chose H_2O_2 irradiation to generate $^\bullet$OH instead of e.g. the dark Fenton reaction, because the latter process yields a highly oxidised Fe-H_2O_2 adduct (often indicated as ferryl) that only partially evolves into $^\bullet$OH, depending on pH (Pignatello et al., 1999; Bossmann et al., 2004). Moreover, ferryl is reactive on its own and its reactivity could significantly bias the kinetics of the studied processes and the formation yields of intermediates (Bossmann et al., 1998).

3.1.3. Reaction of IBP with irradiated AQ2S

Figure 2c reports the time evolution of IBP and IBAP upon UVA irradiation of 0.1 mM AQ2S, chosen as CDOM proxy for reasons described before. The direct photolysis of IBP was negligible under such irradiation conditions, likely because of low to negligible UVA absorption by IBP. Therefore, the photochemistry of the system would be dominated by AQ2S triplet state, ^{3}AQ2S* (Maddigapu et al., 2010; Bedini et al., 2012). From experimental data one gets $\eta^{IBP \to IBAP}_{^3AQ2S*} = r'_{IBAP} (r_{IBP})^{-1} = 0.31 \pm 0.04$ at pH 7.2. The yield with AQ2S had a slight pH trend, with values in the range of 0.20-0.25 at pH 2-3 and no significant variation above pH 5. This means that anionic IBP would yield IBAP with slightly higher yield than protonated IBP. Table 1 summarises

the IBAP yields from IBP under neutral conditions, upon direct photolysis and reaction with $^\bullet$OH and ^{3}AQ2S*.

3.2. IBAP phototransformation (irradiation experiments)

The phototransformation kinetics of IBAP was studied *via* the photochemical pathways that could potentially be important in surface waters, namely direct photolysis and reactions with $^\bullet$OH, $CO_3^{-\bullet}$, $^1O_2$ and ^{3}CDOM*. The relevant results are reported below and summarised in Table 1, which reports direct photolysis quantum yield and reaction rate constants of IBAP.

3.2.1. IBAP direct photolysis

IBAP (initial concentration 20 µM) was irradiated under the TL 20W/01 RS lamp (emission maximum at 313 nm, see Figure 1a) at pH 7. The pseudo-first order transformation kinetics had initial rate r_{IBAP} = $(4.23\pm0.95)\times10^{-10}$ M s^{-1}, with an absorbed photon flux $P_a^{IBAP} = \int_\lambda p°(\lambda)\,[1-10^{-\varepsilon_{IBAP}(\lambda)\,b\,[IBAP]}]d\lambda$ = 8.45×10^{-9} Einstein L^{-1} s^{-1}. In the integral, $p°(\lambda)$ is the incident spectral photon flux density of the lamp, $\varepsilon_{IBAP}(\lambda)$ the molar absorption coefficient of IBAP (see Figure 1a), b = 0.4 cm the optical path length in solution, and [IBAP] = 20 µM. From these data it is possible to obtain the polychromatic photolysis quantum yield Φ_{IBAP} = $r_{IBAP}\,(P_a^{IBAP})^{-1}$ = $(5.01\pm1.13)\times10^{-2}$. Note that negligible IBAP transformation took place in the dark, over a time scale comparable to the irradiation experiment.

3.2.2. Reaction between IBAP and $^\bullet$OH

The reaction rate constant between IBAP and $^\bullet$OH was determined upon competition kinetics with 2-propanol, using H_2O_2 photolysis as $^\bullet$OH source. This approach was preferred over the comparison of IBAP degradation with a reference compound in the same solution, because in the latter case the low-concentration data points (high reaction times) would greatly influence the rate constant value. These points are affected by large experimental error, while in the present case the initial rates depend on high-concentration points where the error is much lower. Figure 3 reports r_{IBAP} *vs.* [2-Propanol], upon UVB irradiation of 1 mM H_2O_2 + 20 µM IBAP at pH 7. Note that IBAP direct photolysis would account for less than 6% of IBAP transformation under these conditions, which is lower than the uncertainty on the rates and can be neglected. The following reactions would be involved in the transformation of IBAP upon H_2O_2 irradiation (Buxton et al., 1988):

$$H_2O_2 + h\nu \rightarrow 2\ ^\bullet OH \qquad\qquad [r_{\bullet OH}] \qquad\qquad (1)$$
$$2\text{-Propanol} + {}^\bullet OH \rightarrow \text{Products} \qquad [k_2 = 1.9\times10^9\ M^{-1}\ s^{-1}] \qquad (2)$$
$$IBAP + {}^\bullet OH \rightarrow \text{Products} \qquad\quad [k_3] \qquad\qquad (3)$$
$$H_2O_2 + {}^\bullet OH \rightarrow HO_2^\bullet + H_2O \qquad [k_4 = 2.7\times10^7\ M^{-1}\ s^{-1}] \qquad (4)$$

Upon application of the steady-state approximation to $^\bullet OH$, one gets the following expression for the transformation rate of IBAP (r_{IBAP}) as a function of [2-Propanol]:

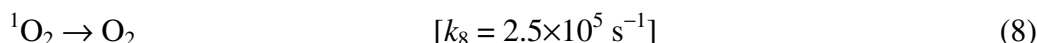$$r_{IBAP} = r_{\bullet OH} \frac{k_3 [IBAP]}{k_3 [IBAP] + k_2 [2 - \text{Propanol}] + k_4 [H_2O_2]} \qquad (5)$$

where $r_{\bullet OH}$ is the formation rate of $^\bullet OH$ in reaction (1). The fit of the rate data of Figure 2 with equation (5) yielded $k_3 = (2.0 \pm 0.5) \times 10^{10}$ M^{-1} s^{-1}. This value will be adopted as the second-order reaction rate constant of $^\bullet OH$ with IBAP. The comparison of the reaction rate constants with $^\bullet OH$ of IBAP, 2-propanol and H_2O_2 suggests that <7% $^\bullet OH$ would react with H_2O_2 to form the poorly reactive species $HO_2^\bullet/O_2^{-\bullet}$, while >93% $^\bullet OH$ would react with IBAP and 2-propanol. This issue excludes any $HO_2^\bullet/O_2^{-\bullet}$-related bias in the studied system. Note that $r_{\bullet OH} = (7.0 \pm 0.5) \times 10^{-9}$ M s^{-1} and that, in the absence of 2-propanol, it is $[^\bullet OH] = \dfrac{r_{\bullet OH}}{k_3 [IBAP] + k_4 [H_2O_2]} = (1.8 \pm 0.6) \times 10^{-14}$ M.

3.2.3. Reaction between IBAP and $CO_3^{-\bullet}$

The importance of the reaction between IBAP and $CO_3^{-\bullet}$ for surface waters was assessed by means of a screening approach that makes use of nitrate irradiation in the presence of bicarbonate. The rationale of the method is that nitrate photolysis initially yields $^\bullet OH + ^\bullet NO_2$, surrounded by a cage of water molecules. The two photofragments can either recombine or diffuse into the solution bulk, where they react with other species. NaHCO$_3$ addition enables the scavenging of $^\bullet OH$ by HCO_3^- and CO_3^{2-} to yield $CO_3^{-\bullet}$, which is reactive but less than $^\bullet OH$. However, if the concentration of added NaHCO$_3$ is sufficiently high, HCO_3^- and CO_3^{2-} can also react with cage $^\bullet OH$ and inhibit the recombination between $^\bullet OH$ and $^\bullet NO_2$ within the cage. Indeed, the water molecules surrounding the photogenerated fragments ($^\bullet OH + ^\bullet NO_2$) favour the geminate fragment recombination to nitrate and H$^+$, which is in competition with diffusion in the solution bulk (Nissenson et al., 2010). However, if cage $^\bullet OH$ is consumed by bicarbonate (which, at sufficiently high concentration, can replace some of the cage H_2O molecules), recombination is no longer operational. Because of the inhibition of cage recombination, the formation rate of $CO_3^{-\bullet}$ at high bicarbonate is higher than the formation rate of $^\bullet OH$ without bicarbonate. The formation of a higher amount of a less reactive species has variable effects depending on substrate reactivity towards $^\bullet OH$ and $CO_3^{-\bullet}$: bicarbonate inhibits the degradation of compounds that do not react with $CO_3^{-\bullet}$ to a significant extent. Conversely, it enhances transformation of compounds undergoing important reaction with $CO_3^{-\bullet}$ in both laboratory systems and surface waters (Vione et al., 2009). On this basis, the bicarbonate effect on nitrate-induced photodegradation was tested for IBAP and the observed inhibition suggests that reaction between IBAP and $CO_3^{-\bullet}$ would not be important. Detailed experimental results are reported as SM.

3.2.4. Reaction between IBAP and $^1O_2$

The initial transformation rate of IBAP (r_{IBAP}), with initial concentration varied in the range of 5-50 µM, was studied at pH 7 upon irradiation of 10 µM Rose Bengal (RB) as $^1O_2$ source (Miller, 2005). The plot of r_{IBAP} vs. initial IBAP concentration followed a linear trend (see SM, Figure S2), which could be fitted with the equation $r_{IBAP} = (1.48\pm0.14)\times10^{-5}$ [IBAP]. In the experimental system, the reaction between IBAP and $^1O_2$ is in competition with $^1O_2$ thermal deactivation (Rodgers and Snowden, 1982). The following reaction scheme applies to RB and IBAP under irradiation:

$$RB + h\nu + O_2 \rightarrow RB + {}^1O_2 \qquad\qquad (6)$$

$$IBAP + {}^1O_2 \rightarrow Products \qquad [k_7] \qquad\qquad (7)$$

$$^1O_2 \rightarrow O_2 \qquad [k_8 = 2.5\times10^5 \text{ s}^{-1}] \qquad\qquad (8)$$

Upon application of the steady-state approximation to $^1O_2$ one gets the following expression for r_{IBAP}:

$$r_{IBAP} = \frac{R_{^1O_2} \, k_{16} \, [IBAP]}{k_{17} + k_{16} \, [IBAP]} \qquad\qquad (9)$$

where $r_{^1O_2} = (1.61\pm0.02)\times10^{-6}$ M s^{-1} is the formation rate of $^1O_2$ by 10 µM RB under the irradiation device (determined upon irradiation of 10 µM RB + 0.1 mM furfuryl alcohol, see Figure S3 in SM and related discussion). For very low [IBAP] ($k_7\times$[IBAP] $\ll k_8$) one gets:

$$\lim_{[IBAP]\to 0}\{r_{IBAP}\} = r_{^1O_2} \cdot k_7 \cdot k_8^{-1} \cdot [IBAP] \qquad\qquad (10)$$

Equation (10) is consistent with the linear trend of r_{IBAP} vs. [IBAP] determined experimentally. From equation (10) and the experimental data one derives $r_{IBAP}\,[IBAP]^{-1} = r_{^1O_2}\,k_{16}\,k_{17}^{-1} = (1.48\pm0.14)\times10^{-5}$. From the known values of $r_{^1O_2}$ and k_8 one gets $k_7 = (2.29\pm0.25)\times10^6$ M^{-1} s^{-1} as the reaction rate constant between IBAP and $^1O_2$. It is also $[^1O_2] = r_{^1O_2} \times k_8^{-1} = (6.4\pm0.1)\times10^{-12}$ M. A process that could possibly interfere with the degradation of IBAP is the reaction between IBAP itself and $^3RB^*$. Indeed, formation of $^3RB^*$ followed by reaction with O_2 is required for $^1O_2$ generation to take place. However, if part of the (very limited) IBAP degradation occurs with $^3RB^*$ and not with $^1O_2$, this means that the already low (and environmentally negligible, *vide infra*) reaction rate constant between IBAP and $^1O_2$ is overestimated. It only adds evidence to the lack of environmental importance of the reaction between IBAP and $^1O_2$.

3.2.5. Reaction of IBAP with irradiated AQ2S

IBAP (initial concentration in the 2-20 µM range) was UVA irradiated in the presence of 0.1 mM AQ2S at pH 7. Direct photolysis (irradiation without AQ2S) was negligible under the chosen experimental conditions (irradiation time ≤1h). It was obtained $r_{IBAP} = (6.74\pm0.25)\times10^{-4}$ [IBAP] (see also SM, Figure S4).

The transformation of IBAP by irradiated AQ2S is most likely accounted for by reaction with $^3AQ2S^*$. Upon application of the steady-state approximation to $^3AQ2S^*$ (Sur et al., 2012) one can

obtain the following expression for IBAP photodegradation rate (see SM for the derivation of equation (11)):

$$r_{IBAP} = \Phi_{^3AQ2S*} \, P_a^{AQ2S} \cdot \frac{k_{^3AQ2S*,IBAP} \, [IBAP]}{k_{^3AQ2S*} + k_{^3AQ2S*,IBAP} \, [IBAP]} \tag{11}$$

where $\Phi_{^3AQ2S*}$ = 0.18 is the quantum yield of triplet formation (Alegría et al., 1999), $k_{^3AQ2S*}$ = 1.1×10^7 s^{-1} is the first-order rate constant of triplet deactivation (Loeff et al., 1983), $k_{^3AQ2S*,IBAP}$ is the second-order reaction rate constant between IBAP and ^{3}AQ2S*, and P_a^{AQ2S} is the photon flux absorbed by 0.1 mM AQ2S in the irradiated solution. At low [IBAP] it is $k_{^3AQ2S*,IBAP} \times$[IBAP] « $k_{^3AQ2S*}$, and equation (11) can be linearised in agreement with experimental data:

$$\frac{r_{IBAP}}{[IBAP]} = \frac{\Phi_{^3AQ2S*} \, P_a^{AQ2S} \, k_{^3AQ2S*,IBAP}}{k_{^3AQ2S*}} \tag{12}$$

Absorption of lamp radiation by IBAP would be negligible compared to AQ2S: for instance, at 330 nm the absorbance of AQ2S is ~600 times higher than for IBAP. Therefore, P_a^{AQ2S} can be simply calculated as follows:

$$P_a^{AQ2S} = \int_\lambda p°(\lambda) \, [1 - 10^{-\varepsilon_{AQ2S}(\lambda)bc_{AQ2S}}] \, d\lambda \tag{13}$$

where $\varepsilon_{AQ2S}(\lambda)$ is the molar absorption coefficient of AQ2S (see Figure 1c), b = 0.4 cm the optical path length in solution, and c_{AQ2S} = 0.1 mM is the initial concentration of AQ2S. Numerical integration of equation (13) yields P_a^{AQ2S} = 2.23×10^{-6} Einstein L^{-1} s^{-1}. When considering equation (12), the experimental results ($r_{IBAP} [IBAP]^{-1} = (6.74 \pm 0.25) \times 10^{-4}$) and the known values of $\Phi_{^3AQ2S*}$, $k_{^3AQ2S*}$ and P_a^{AQ2S}, one obtains $k_{^3AQ2S*,IBAP}$ = $(1.85 \pm 0.07) \times 10^{10}$ M^{-1} s^{-1} as the reaction rate constant between ^{3}AQ2S* and IBAP. This finding confirms that the hypothesis $k_{^3AQ2S*,IBAP}$ [IBAP] « $k_{^3AQ2S*}$ was correct. Note that, under such conditions, it would be [^{3}AQ2S*] = $\Phi_{^3AQ2S*}$ P_a^{AQ2S} $(k_{^3AQ2S*})^{-1}$ = 3.6×10^{-14} M. Hereafter, the value of $k_{^3AQ2S*,IBAP}$ will be taken as representative of the reaction rate constant(s) between IBAP and the excited triplet states of CDOM (^{3}CDOM*).

3.3. Photochemical modelling

Table 1 reports IBAP phototransformation parameters and formation yields from IBP. Moreover, literature data of IBP phototransformation (Vione et al., 2011) are also reported. Such data set, with ^{3}AQ2S* entries assumed as representative of ^{3}CDOM*, allows the modelling of: *(i)* IBP phototransformation in surface waters (pseudo first-order rate constant k_{IBP} or half-life time τ_{IBP}); *(ii)* IBAP formation from IBP (rate constant k'_{IBAP} and formation yield $\eta_{tot}^{IBP \to IBAP}$), and *(iii)* IBAP photoinduced transformation (rate constant k_{IBAP}), mostly accounted for by photolysis and reaction with $^\bullet$OH and ^{3}CDOM*.

3.3.1. Formation/transformation kinetics

Model results concerning IBAP and IBP phototransformation are reported as SM (Figures S5 and S7, respectively). Briefly, the model predicts that IBAP is less persistent than IBP. Considering the ratio of degradation rate constants, one has $k_{IBAP} \ k_{IBP}^{-1} \sim 1.5$ under low-DOC conditions and $k_{IBAP} \ k_{IBP}^{-1} \sim 1.8$-1.9 at high DOC.

Figure 4a,b reports the first-order rate constant of IBAP formation, k'_{IBAP}, as a function of DOC and depth d. The plots were generated by using the *Plotgraph* function of the APEX software. Model uncertainty was around 30-35%, depending on errors on measured kinetic data (Table 2) and on model parameters (Al Housari et al., 2010). It was calculated by using the *APEX_Errors* function of the APEX software. Figures 4a and 4b differ for the d range, which is respectively 0-2 m (4a) and 3-8 m (4b). The decrease of k'_{IBAP} with increasing d, which is evident in both cases, is due to the fact that the bottom layers of a deep water body are poorly illuminated by sunlight: deep water environments are less favourable to photochemical processes than shallow ones. At the lower d values (Figure 4a), one can see that increasing DOC would favour IBAP formation. Because high occurrence of CDOM is expected when DOC is high (Rostan and Cellot, 1995), the k'_{IBAP} increase would be accounted for by the enhancement of ^{3}CDOM* reactions that produce IBAP with high yield (0.31±0.04).

Competition between IBP and CDOM for sunlight irradiance is expected to inhibit the direct photolysis of IBP. The extent of such an inhibition would be higher at high CDOM (and, therefore, high DOC) and high d, because of higher water absorbance and higher degree of absorption saturation. In particular, the minimum of k'_{IBAP} *vs.* DOC at high d (Figure 4b) is accounted for by the fact that direct photolysis is more important at low DOC and ^{3}CDOM* reaction at high DOC. Therefore, the main DOC effect would be inhibition of IBP photolysis before the minimum, and enhancement of ^{3}CDOM* reaction after the minimum. Note that nitrate and nitrite ($^\bullet$OH sources) and carbonate and bicarbonate ($^\bullet$OH scavengers) have little to negligible effect on k'_{IBAP}, because $^\bullet$OH plays a minor role in IBAP formation.

3.3.2. IBAP formation yields

Figure 4c,d reports the yield of IBAP formation from IBP, $\eta_{tot}^{IBP \to IBAP}$, as a function of nitrite and d and as a function of DOC and d. Note that $\eta_{tot}^{IBP \to IBAP} = \dfrac{k'_{IBAP}}{k_{IBP}} \approx$

$$\approx \frac{\eta_{\bullet OH}^{IBP \to IBAP} \ k_{\bullet OH}^{IBP} + \eta_{Phot}^{IBP \to IBAP} \ k_{Phot}^{IBP} + \eta_{^3CDOM*}^{IBP \to IBAP} \ k_{^3CDOM*}^{IBP}}{k_{\bullet OH}^{IBP} + k_{Phot}^{IBP} + k_{^3CDOM*}^{IBP}}$$ (De Laurentiis et al., 2012). The value of

$\eta_{tot}^{IBP \to IBAP}$ slightly decreases with increasing nitrite, because NO_2^- enhances the $^\bullet$OH pathway that produces IBAP with low yield. Increasing d slightly enhances $\eta_{tot}^{IBP \to IBAP}$, because it favours the ^{3}CDOM* pathway that has the highest IBAP yield. Moreover, at high d, competition for irradiance

between nitrate, nitrite, IBP and CDOM (which is by far the main radiation absorber at 300-500 nm; Bracchini et al., 2004) would inhibit both direct photolysis and $^\bullet$OH reaction. Similar issues of ^{3}CDOM* enhancement *vs.* photolysis and $^\bullet$OH account for the increase of $\eta_{tot}^{IBP \to IBAP}$ with increasing DOC (Figure 4d), due to the replacement of lower-yield processes with ^{3}CDOM*.

3.3.3. Implications for IBAP occurrence in surface waters

The data of k_{IBP}, k'_{IBAP} and k_{IBAP} derived from the model (where k denotes degradation and k' means formation) allow the prediction of IBP and IBAP environmental concentration values, resulting from photochemical reactions. The first tested scenario considers an initial IBP spike with concentration c_o^{IBP}, sufficiently low to prevent IBP from affecting the steady-state [$^\bullet$OH] and [^{3}CDOM*]. IBP would undergo degradation, including transformation into IBAP that would be degraded as well. Under these circumstances, and if $c_o^{IBAP} = 0$, the following trends of IBP and IBAP concentration as a function of time t would be obtained:

$$c^{IBP} = c_o^{IBP}\, e^{-k_{IBP}\, t} \tag{14}$$

$$c^{IBAP} = \frac{k'_{IBAP}\, c_o^{IBP}}{k_{IBAP} - k_{IBP}} (e^{-k_{IBP}\, t} - e^{-k_{IBAP}\, t}) \tag{15}$$

Figure 5 reports the time trends of IBP and IBAP under four different scenarios, which influence the modelled values of k_{IBP}, k'_{IBAP} and k_{IBAP}: ① d = 1 m and DOC = 1 mg C L^{-1}; ② d = 1 m and DOC = 10 mg C L^{-1}; ③ d = 10 m and DOC = 1 mg C L^{-1}; ④ d = 10 m and DOC = 10 mg C L^{-1}. Other conditions for all cases were 0.1 mM nitrate, 1 μM nitrite, 10 μM carbonate and 2 mM bicarbonate. It can be seen that d is the most important factor to influence the persistence of both compounds. The maximum concentration value reached by IBAP, c_{max}^{IBAP} (6-8% of c_o^{IBP}, lower for ① and higher for ④) would be little influenced by environmental conditions. In fact, the higher k_{IBAP} k_{IBP}^{-1} ratio at high DOC (faster IBAP degradation compared to IBP) would be largely offset by higher $\eta_{tot}^{IBP \to IBAP}$ (higher IBAP formation yield from IBP). Environmental exposure to elevated IBAP values would be higher under scenarios ③ and ④, because of higher IBAP persistence. Figure 5 refers to summertime conditions, and the degradation kinetics of both IBP and IBAP would be slower in other seasons. However, rate constant ratios and c_{max}^{IBAP} values undergo more limited seasonal variations. The seasonal variation of the degradation kinetics can be approximately assessed by means of the *APEX_Season* function. Depending on water chemistry conditions, the half-life times of IBP and IBAP are 5-9 times longer in January than in July.

In many environmental circumstances there would not be a single IBP spike but rather a fairly continuous emission into surface waters. Assume a very simplified case in which IBP has a constant concentration value c_{const}^{IBP}, resulting from the emission/attenuation budget. If photochemistry is the only important transformation process for both IBP and IBAP, under photochemical steady-state conditions (IBAP concentration also constant) one has:

$$c_{const}^{IBAP} = \frac{k'_{IBAP}}{k_{IBAP}} c_{const}^{IBP} \qquad (16)$$

In the same d and DOC scenarios as for ①-④ one obtains c_{const}^{IBAP} = 0.14-0.16 c_{const}^{IBP} (the value of 0.16 refers to scenario ④). The associated uncertainty (σ level), assessed with the *APEX_Errors* function, is around 30-40%. IBAP has been detected at various stages in wastewater treatment plants (WWTPs) (Zorita et al., 2009), but the IBAP/IBP ratio was always considerably lower than 0.14-0.16. Therefore, photoreactions could increase the IBAP/IBP ratio in surface waters compared to WWTP outlets.

In this paper, reactivity data with ^{3}AQ2S* were assumed to be representative of ^{3}CDOM* (see above for the rationale). It is possible that reactivity of ^{3}AQ2S* overestimates that of ^{3}CDOM*, thus we checked the robustness of conclusions based on such assumption. We assessed the effect of varying the rate constant values of IBP and IBAP with ^{3}CDOM*, as well as varying IBAP yields from IBP. The relevant calculations are reported as SM and they show that, under almost all tested scenarios, IBAP would still be a major transformation intermediate of IBP.

Interpretation of model results in the light of the available literature suggests that IBAP could be an intermediate of concern in water environments where IBP concentration values are in the µg L^{-1} range (Gros et al., 2007; Xu et al., 2011; Stasinakis et al., 2012; Chen et al., 2012). Conversely, IBAP is unlikely to cause problems where IBP values are in the ng L^{-1} range (Gros et al., 2007; Zorita et al., 2007; Xu et al., 2011; Stasinakis et al., 2012; Chen et al., 2012).

4. Conclusions

- Harmful IBAP can be formed *via* all three major pathways of IBP phototransformation in the environment: direct photolysis and reaction with $^\bullet$OH and ^{3}CDOM*. IBAP formation yields from IBP are lowest with $^\bullet$OH and highest with ^{3}CDOM*. Because of faster IBAP phototransformation compared to IBP, the ratio of phototransformation rate constants, k_{IBAP} k_{IBP}^{-1}, would vary in the range 1.5-1.9 (lower at low DOC and higher at high DOC).

- According to our photochemical model the concentration values reached by IBAP in surface waters could be up to ~15% of the IBP ones. In this case, the IBAP/IBP ratio would be little influenced by environmental variables.

- Our data show that IBAP formation could be an important process in IBP environmental chemistry. In water environments where IBP concentration values are in the ng L^{-1} range, the resulting IBAP levels are unlikely to cause much concern. However, the scenario might significantly differ under circumstances where IBP is in the µg L^{-1} or even in the tens µg L^{-1} range. In such cases, IBAP should be monitored to assess the environmental impact of IBP. The results of this work call for the need to increase the very limited knowledge that is currently available about IBAP occurrence in surface waters.

REFERENCES

Achilleos, A., Hapeshi, E., Xekoukoulotakis, N. P., Mantzavinos, D., Fatta-Kassinos, D., 2010. UV-A and solar photodegradation of ibuprofen and carbamazepine catalyzed by TiO_2. Separation Science and Technology 45, 1564-1570.

Al Housari, F., Vione, D., Chiron, S., Barbati, S., 2010. Reactive photoinduced species in estuarine waters. Characterization of hydroxyl radical, singlet oxygen and dissolved organic matter triplet state in natural oxidation process. Photochemical and Photobiological Sciences 9, 78-86.

Alegría, A.E., Ferrer, A., Santiago, G., Sepúlveda, E., Flores, W., 1999. Photochemistry of water-soluble quinones. Production of the hydroxyl radical, singlet oxygen and the superoxide ion. Journal of Photochemistry and Photobiology A: Chemistry 127, 57-65.

Andreozzi, R., Marotta, R., Nicklas, P., 2003. Pharmaceuticals in STP effluents and their solar photodegradation in aquatic environment. Chemosphere 50, 1319-1330.

Bedini, A., De Laurentiis, E., Sur, B., Maurino, V., Minero, C., Brigante, M., Mailhot, G., Vione, D., 2012. Phototransformation of anthraquinone-2-sulphonate in aqueous solution. Photochemical and Photobiological Sciences 11, 1445-1453.

Boreen, A. L., Arnold, W. A., McNeill, K., 2003. Photodegradation of pharmaceuticals in the aquatic environment: A review. Aquatic Sciences 65, 320-341.

Bossmann, S. H., Oliveros, E., Gob, S., Siegwart, S., Dahlen, E. P., Payawan, L., Straub, M., Worner, M., Braun, A. M., 1998. New evidence against hydroxyl radicals as reactive intermediates in the thermal and photochemically enhanced fenton reactions. Journal of Physical Chemistry A 102, 5542-5550.

Bossmann, S. H., Oliveros, E., Kantor, M., Niebler, S., Bonfill, A., Shahin, N., Worner, M., Braun, A. M., 2004. New insights into the mechanisms of the thermal Fenton reactions occurring using different iron(II)-complexes. Water Science and Technology 49, 75-80.

Bracchini, L., Loiselle, S., Dattilo, A. M., Mazzuoli, S., Cozar, A., Rossi, C., 2004. The spatial distribution of optical properties in the ultraviolet and visible in an aquatic ecosystem. Photochemistry and Photobiology 80, 139-149.

Buser, H., Poiger, T., Müller, M. D., 1999. Occurrence and environmental behavior of the chiral pharmaceutical drug ibuprofen in surface waters and in wastewater. Environmental Science and Technology 33, 2529-2535.
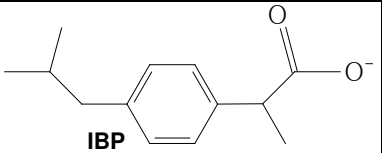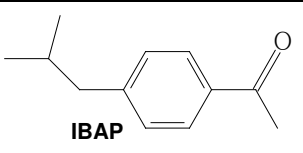
Buxton, G. V., Greenstock, C. L., Helman, W. P., Ross, A. B., 1988. Critical review of rate constants for reactions of hydrated electrons, hydrogen atoms and hydroxyl radicals ($^{\bullet}$OH/$^{\bullet}$O$^-$) in aqueous solution. Journal of Physical and Chemical Reference Data 17, 1027-1284.

Camacho-Munoz, D., Martin, J., Santos, J. L., Aparicio, I., Alonso, E., 2010. Occurrence, temporal evolution and risk assessment of pharmaceutically active compounds in Donana Park (Spain). Journal of Hazardous Materials 183, 602-608.

Canonica, S., Kohn, T., Mac, M., Real, F. J., Wirz, J., Von Gunten, U., 2005. Photosensitizer method to determine rate constants for the reaction of carbonate radical with organic compounds. Environmental Science and Technology 39, 9182-9188.

Canonica, S., Freiburghaus, M., 2001. Electron-rich phenols for probing the photochemical reactivity of freshwaters. Environmental Science and Technology 35, 690-695.

Carballa, M., Omil, F., Lema, J. M., Llompart, M., Garcia-Jares, C., Rodriguez, I., Gomez, M., Ternes, T., 2004. Behavior of pharmaceuticals, cosmetics and hormones in a sewage treatment plant. Water Research 38, 2918-2926.

Castell, J. V., Gomez, M. J., Miranda, M. A., Morera, I. M., 1987. Photolytic degradation of ibuprofen – Toxicity of the isolated photoproducts on fibroblasts and erythrocytes. Photochemistry and Photobiology 46, 991-996.

Castiglioni, S., Bagnati, R., Fanelli, R., Pomati, F., Calamari, D., Zuccato, E., 2006. Removal of pharmaceuticals in sewage treatment plants in Italy. Environmental Science and Technology 40, 357-363.

Chen, H., Li, X. J., Zhu, S. C., 2012. Occurrence and distribution of selected pharmaceuticals and personal care products in aquatic environments: A comparative study of regions in China with different urbanization levels. Environmental Science and Pollution Research 19, 2381-2389.

Choina, J., Kosslick, H., Fischer, C., Flechsig, G. U., Frunza, L., Schulz, A., 2013. Photocatalytic decomposition of pharmaceutical ibuprofen pollutions in water over titania catalyst. Applied Catalysis B: Environmental 129, 589-598.

Cory, R. M., McKnight, D. M., 2005. Fluorescence spectroscopy reveals ubiquitous presence of oxidized and reduced quinones in dissolved organic matter. Environmental Science and Technology 39, 8142-8149.

Cory, W. C., Harris, C., Martinez, S., 2010. Accelerated degradation of ibuprofen in tablets. Pharmaceutical Development and Technology 15, 636-643.

De Laurentiis, E., Chiron, S., Kouras-Hadef, S., Richard, C., Minella, M., Maurino, V., Minero, C., Vione, D., 2012. Photochemical fate of carbamazepine in surface freshwaters: Laboratory measures and modeling. Environmental Science and Technology 46, 8164-8173.

Fernandez, C., Gonzalez-Doncel, M., Pro, J., Carbonell, G., Tarazona, J. V., 2010. Occurrence of pharmaceutically active compounds in surface waters of the Henares-Jarama-Tajo river system (Madrid, Spain) and a potential risk characterization. Science of the Total Environment 408, 543-551.

Gros, M., Petrovic, M., Barceló, D., 2007. Wastewater treatment plants as a pathway for aquatic contamination by pharmaceuticals in the Ebro river basin (Northeast Spain). Environmental Toxicology and Chemistry 26, 1553-1562.

Huang, J., Mabury, S. A., 2000. The role of carbonate radical in limiting the persistence of sulfur-containing chemicals in sunlit natural waters. Chemosphere 41, 1775-1782.

Jacobs, L. E., Fimmen, R. L., Chin, Y. P., Mash, H. E., Weavers, L. K., 2011. Fulvic acid mediated photolysis of ibuprofen in water. Water Research 45, 4449-4458.

Kanabar, D., Dale, S., Rawat, M., 2007. A review of ibuprofen and acetaminophen use in febrile children and the occurrence of asthma- related symptoms. Clinical Therapeutics 29, 2716-2723.

Kuhn, H. J., Braslavsky, S. E., Schmidt, R., 2004. Chemical actinometry. Pure and Applied Chemistry 76, 2105-2146.

Kunkel, U., Radke, M., 2011. Reactive tracer test to evaluate the fate of pharmaceuticals in rivers. Environmental Science and Technology 45, 6296-6302.

Lin, A. Y. C., Plumlee, M. H., Reinhard, M., 2006. Natural attenuation of pharmaceuticals and alkylphenol polyethoxylate metabolites during river transport: Photochemical and biological transformation. Environmental Toxicology and Chemistry 25, 1458-1464.

Loeff, I., Treinin, A., Linschitz, H., 1983. Photochemistry of 9,10-anthraquinone-2-sulfonate in solution. 1. Intermediates and mechanism. Journal of Physical Chemistry 87, 2536-2544.

Maddigapu, P. R., Bedini, A., Minero, C., Maurino, V., Vione, D., Brigante, M., Mailhot, G., Sarakha, M., 2010. The pH-dependent photochemistry of anthraquinone-2-sulfonate. Photochemical and Photobiological Sciences 9, 323-330.

Maddigapu, P. R., Minella, M., Vione, D., Maurino, V., Minero, C., 2011. Modeling phototransformation reactions in surface water bodies: 2,4-Dichloro-6-nitrophenol as a case study. Environmental Science and Technology 45, 209-214.

Marenich, A. V., Cramer, C. J., Truhlar, D. G., 2009. Universal solvation model based on solute electron density and on a continuum model of the solvent defined by the bulk dielectric constant and atomic surface tensions. Journal of Physical Chemistry B 113, 6378-6396.

Martell, A. E., Smith, R. M., Motekaitis, R. J., 1997. Critically selected stability constants of metal complexes database. Version 4.0.

Mendez-Arriaga, F., Esplugas, S., Gimenez, J., 2008. Photocatalytic degradation of non-steroidal anti-inflammatory drugs with TiO_2 and simulated solar irradiation. Water Research 42, 585-594.

Miller, J. S., 2005. Rose-Bengal sensitized photooxidation of 2-chlorophenol in water using solar simulated light. Water Research 39, 412-422.

Miranda, M. A., Morera, I., Vargas, F., Gomezlechon, M. J., Castell, J. V., 1991. In-vitro assessment of the phototoxicity of anti-inflammatory 2-arylpropionic acids. Toxicology in Vitro 5, 451-455.

Miranda-Garcia, N., Suarez, S., Sanchez, B., Coronado, J. M., Malato, S., Maldonado, M. I., 2011. Photocatalytic degradation of emerging contaminants in municipal wastewater treatment plant effluents using immobilized TiO_2 in a solar pilot plant. Applied Catalysis B: Environmental 103, 294-301.

Molinari, R., Pirillo, F., Loddo, V., Palmisano, L., 2006. Heterogeneous photocatalytic degradation of pharmaceuticals in water by using polycrystalline TiO_2 and a nanofiltration membrane reactor. Catalysis Today 188, 205-213.

Mompelat, S., Le Bot, B., Thomas, O., 2009. Occurrence and fate of pharmaceutical products and by-products, from resource to drinking water. Environment International 35, 803-814.

Nissenson, P., Dabdub, D., Das, R., Maurino, V., Minero, C., Vione, D., 2010. Evidence of the water cage effect on the photolysis of NO_3^- and $FeOH^{2+}$. Implications of this effect and of H_2O_2 surface accumulation on photochemistry at the air–water interface of atmospheric droplets. Atmospheric Environment 44, 4859-4866.

Packer, J. L., Werner, J. J., Latch, D. E., McNeill, K., Arnold, W. A., 2003. Photochemical fate of pharmaceuticals in the environment: naproxen, diclofenac, clofibric acid, and ibuprofen. Aquatic Sciences 65, 342-351.

Page, S. E., Arnold, W. A., McNeill, K., 2011. Assessing the contribution of free hydroxyl radical in organic matter-sensitized photohydroxylation reactions. Environmental Science and Technology 45, 2818-2825.

Peuravuori, J., Pihlaja, K., 2009. Phototransformations of selected pharmaceuticals under low-energy UVA-vis and powerful UVB-UVA irradiations in aqueous solutions-the role of natural dissolved organic chromophoric material. Analytical and Bioanalytical Chemistry 394, 1621-1636.

Pignatello, J. J., Liu, D., Huston, P., 1999. Evidence for an additional oxidant in the photoassisted Fenton reaction. Environmental Science and Technology 33, 1832-1839.

Richard, C., ter Halle, A., Brahmia, O., Malouki, M., Halladja, S., 2007. Auto-remediation of surface waters by solar-light: Photolysis of 1-naphthol, and two herbicides in pure and synthetic waters. Catalysis Today 124, 82-87.

Rodgers, M. A. J., Snowden, P. T., 1982. Lifetime of $^1O_2$ in liquid water as determined by time-resolved infrared luminescence measurements. Journal of the American Chemical Society 104, 5541-5543.

Rostan, J. C., Cellot, B., 1995. On the use of UV spectrophotometry to assess dissolved organic carbon origin variations in the Upper Rhône River. Aquatic Sciences 57, 70–80.

Sabri, N., Hanna, K., Yargeau, V., 2012. Chemical oxidation of ibuprofen in the presence of iron species at near neutral pH. Science of the Total Environment 427, 382-389.

Spongberg, A. L., Witter, J. D., Acuna, J., Vargas, J., Murillo, M., Umana, G., Gomez, E., Perez, G., 2011. Reconnaissance of selected PPCP compounds in Costa Rican surface waters. Water Research 45, 6709-6717.

Stasinakis, A. S., Mermigka, S., Samaras, V. G., Farmaki, E., Thomaidis, N. S., 2012. Occurrence of endocrine disrupters and selected pharmaceuticals in Aisonas River (Greece) and environmental risk assessment using hazard indexes. Environmental Science and Pollution Research 19, 1574-1583.

Sur, B., De Laurentiis, E., Minella, M., Maurino, V., Minero, C., Vione, D., 2012. Photochemical transformation of anionic 2-nitro-4-chlorophenol in surface waters: Laboratory and model assessment of the degradation kinetics, and comparison with field data. Science of the Total Environment 426, 3197-3207.

Tixier, C., Singer, H. P., Oellers, S., Muller, S. R., 2003. Occurrence and fate of carbamazepine, clofibric acid, diclofenac, ibuprofen, ketoprofen, and naproxen in surface waters. Environmental Science and Technology 37, 1061-1068.

Vione, D., Khanra, S., Cucu Man, S., Maddigapu, P. R., Das, R., Arsene, C., Olariu, R. I., Maurino, V., Minero, C., 2009. Inhibition vs. enhancement of the nitrate-induced phototransformation of organic substrates by the $^\bullet$OH scavengers bicarbonate and carbonate. Water Research 43, 4718-4728.

Vione, D., Ponzo, M., Bagnus, D., Maurino, V., Minero, C., Carlotti, M. E., 2010. Comparison of different probe molecules for the quantification of hydroxyl radicals in aqueous solution. Environmental Chemistry Letters 8, 95-100.

Vione, D., Maddigapu, P. R., De Laurentiis, E., Minella, M., Pazzi, M., Maurino, V., Minero, C., Kouras, S., Richard, C., 2011. Modelling the photochemical fate of ibuprofen in surface waters. Water Research 45, 6725-6736.

Volonte, M. G., Valora, P. D., Cingolani, A., Ferrara, M., 2005. Stability of ibuprofen in injection solutions. American Journal of Health-System Pharmacy 62, 630-633.

Wu, C. X., Witter, J. D., Spongberg, A. L., Czajkowski, K. P., 2009. Occurrence of selected pharmaceuticals in an agricultural landscape, western Lake Erie basin. Water Research 43, 3407-3416.

Xu, Y., Luo, F., Pal, A., Gin, K. Y. H., Reinhard, M. 2011. Occurrence of emerging organic contaminants in a tropical urban catchment in Singapore. Chemosphere 83, 963-969.

Zorita, S., Barri, T., Mathiasson, L., 2007. A novel hollow-fibre microporous membrane liquid-liquid extraction for determination of free 4-isobutylacetophenone concentration at ultra trace level in environmental aqueous samples. Journal of Chromatography A 1157, 30-37.

Zorita, S., Mårtensson, L., Mathiasson, L., 2009. Occurrence and removal of pharmaceuticals in a municipal sewage treatment system in the south of Sweden. Science of the Total Environment 407, 2760-2770.

Table 1. Kinetic parameters of photochemical processes involving IBP and IBAP in surface waters: direct photolysis quantum yields, reaction rate constants, and transformation yields (note that S means IBP or IBAP where relevant).

|	IBP	IBAP
Φ_S	0.33 ± 0.05 [b]	$(5.01 \pm 1.13) \times 10^{-2}$
$k_{S,^{\bullet}OH}$, $M^{-1}\,s^{-1}$	$(1.0 \pm 0.3) \times 10^{10}$ [b]	$(2.0 \pm 0.5) \times 10^{10}$
$k_{S,^3AQ2S*}$, $M^{-1}\,s^{-1}$ [a]	$(9.7 \pm 0.2) \times 10^9$ [b]	$(1.85 \pm 0.07) \times 10^{10}$
$k_{S,^1O_2}$, $M^{-1}\,s^{-1}$	$(6.0 \pm 0.6) \times 10^4$ [b]	$(2.29 \pm 0.25) \times 10^6$
$k_{S,CO_3^{\bullet-}}$, $M^{-1}\,s^{-1}$	Negligible [b]	Negligible
$\eta_{Phot}^{IBP \rightarrow IBAP}$	0.25 ± 0.07 [c]	
$\eta_{^{\bullet}OH}^{IBP \rightarrow IBAP}$	0.023 ± 0.010 [c]	
$\eta_{^3AQ2S*}^{IBP \rightarrow IBAP}$	0.31 ± 0.04 [c]	

[a] These values are taken as representative of reactivity between IBP and IBAP and ^{3}CDOM*.

[b] The values of these parameters are from Vione et al. (2011). All other values were obtained in this work.

[c] These value are referred to neutral solutions, but negligible variations were observed above pH 5. The different yields observed at pH < 5 are associated with the occurrence of protonated IBP (pK$_a$ = 4.4).
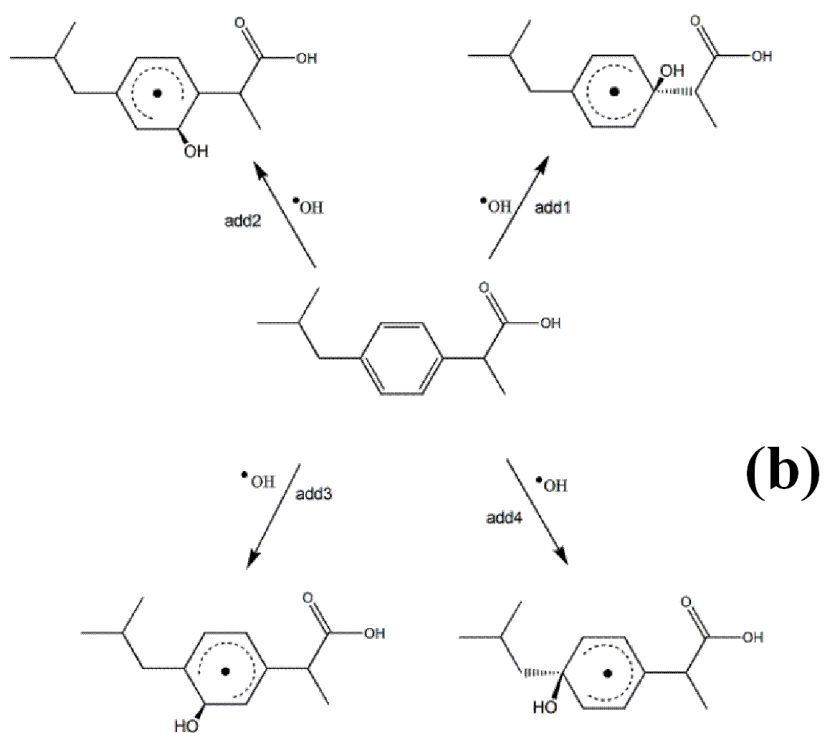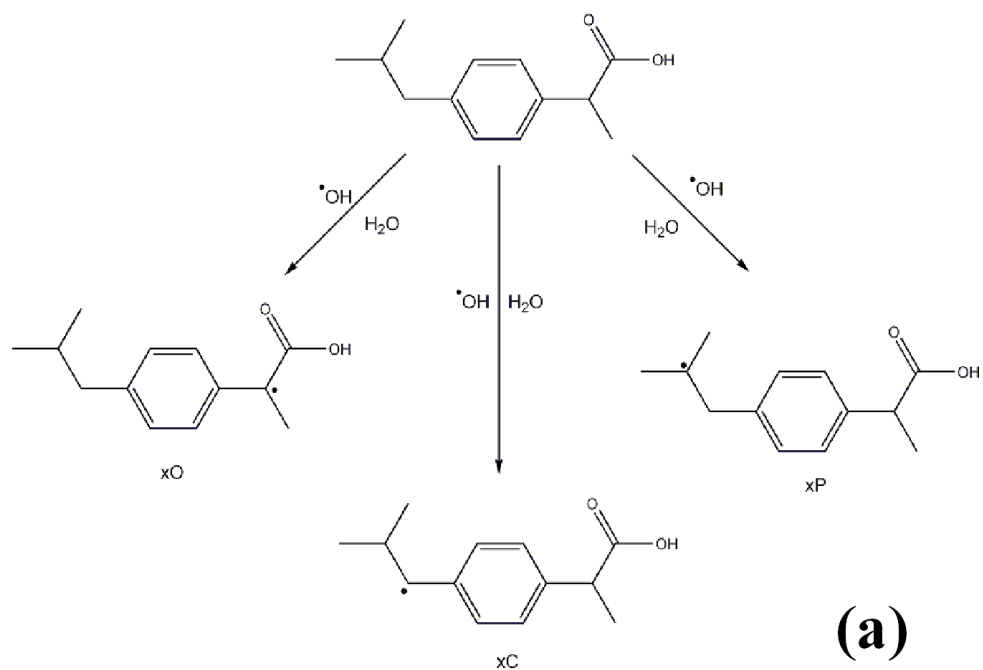
Scheme 1. (a) Hydrogen abstraction pathways in the reaction of IBP with hydroxyl radicals.
(b) Aromatic ring addition pathways in the reaction of IBP with hydroxyl radicals. Calculations were carried out based on the reported reaction scheme.
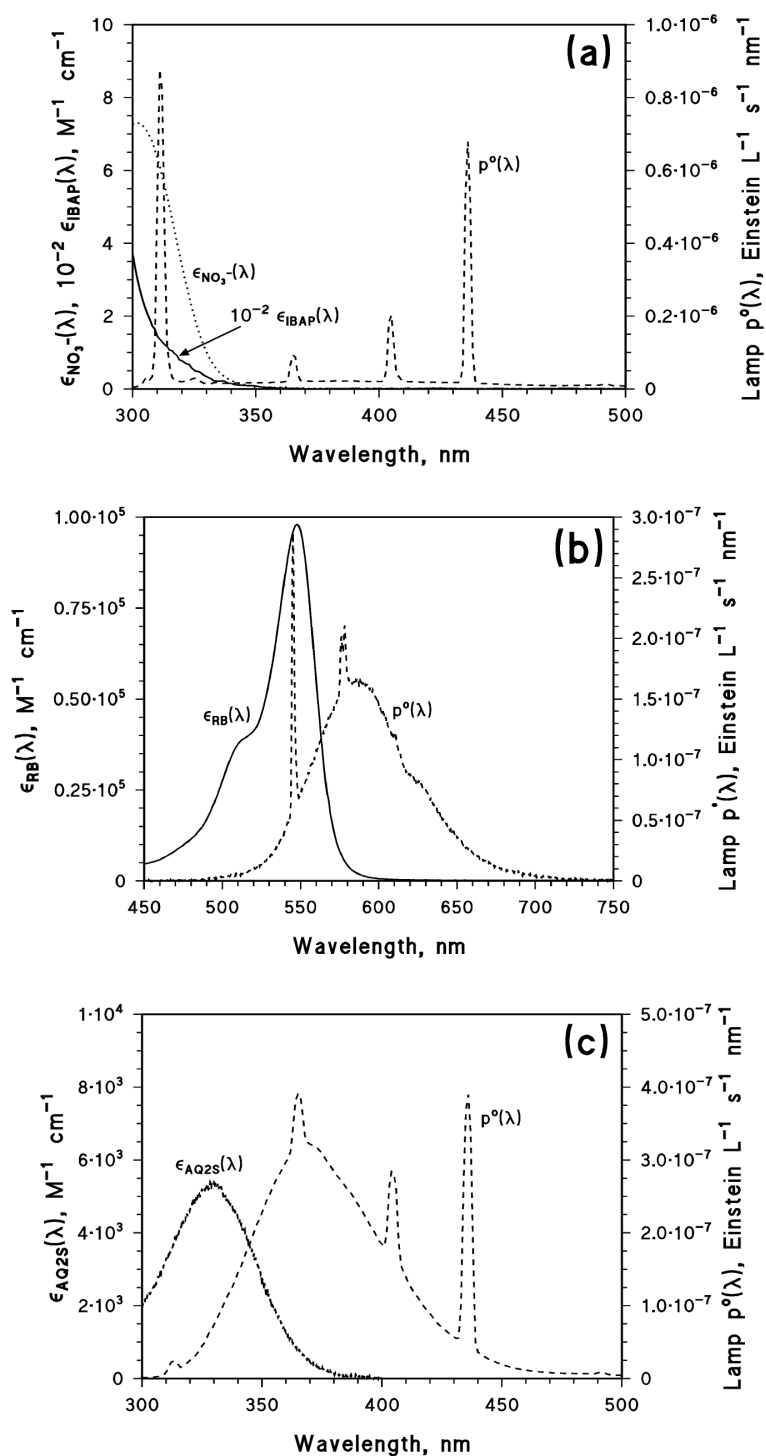
Figure 1. **(a)** Absorption spectra of IBAP and nitrate. Incident spectral photon flux density of the TL 20W/01 RS lamp (UV-Vis, emission maximum at 313 nm).

(b) Absorption spectrum of Rose Bengal (RB). Incident spectral photon flux density of the lamp TL D 18W/16 Yellow.

(c) Absorption spectrum of antraquinone-2-sulphonate (AQ2S). Incident spectral photon flux density of the UVA lamp (TLK 05).
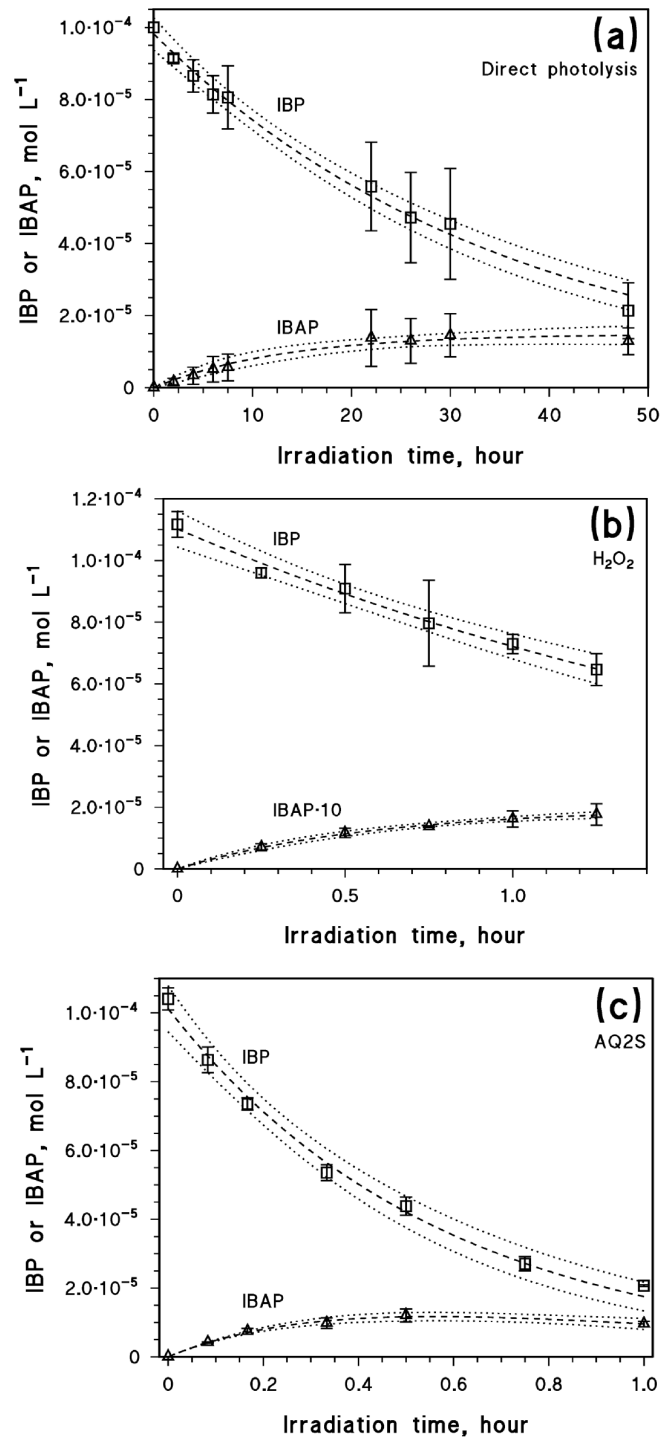
Figure 2. Time trends of IBP and IBAP at pH 7 upon: **(a)** direct UVB photolysis of 20 μM IBP, pH 7; **(b)** UVB irradiation of 20 μM IBP + 1 mM H_2O_2 (pH 7), yielding $^{\bullet}OH$; **(c)** UVA irradiation of 20 μM IBP + 0.1 mM AQ2S, chosen as CDOM proxy. Reported data with error bars (±σ) are the average of replicate runs. The curves fitting the experimental data are dashed, the 95% confidence limits of the fit are dotted. Note that in **(b)** the concentration of IBAP is multiplied by 10.
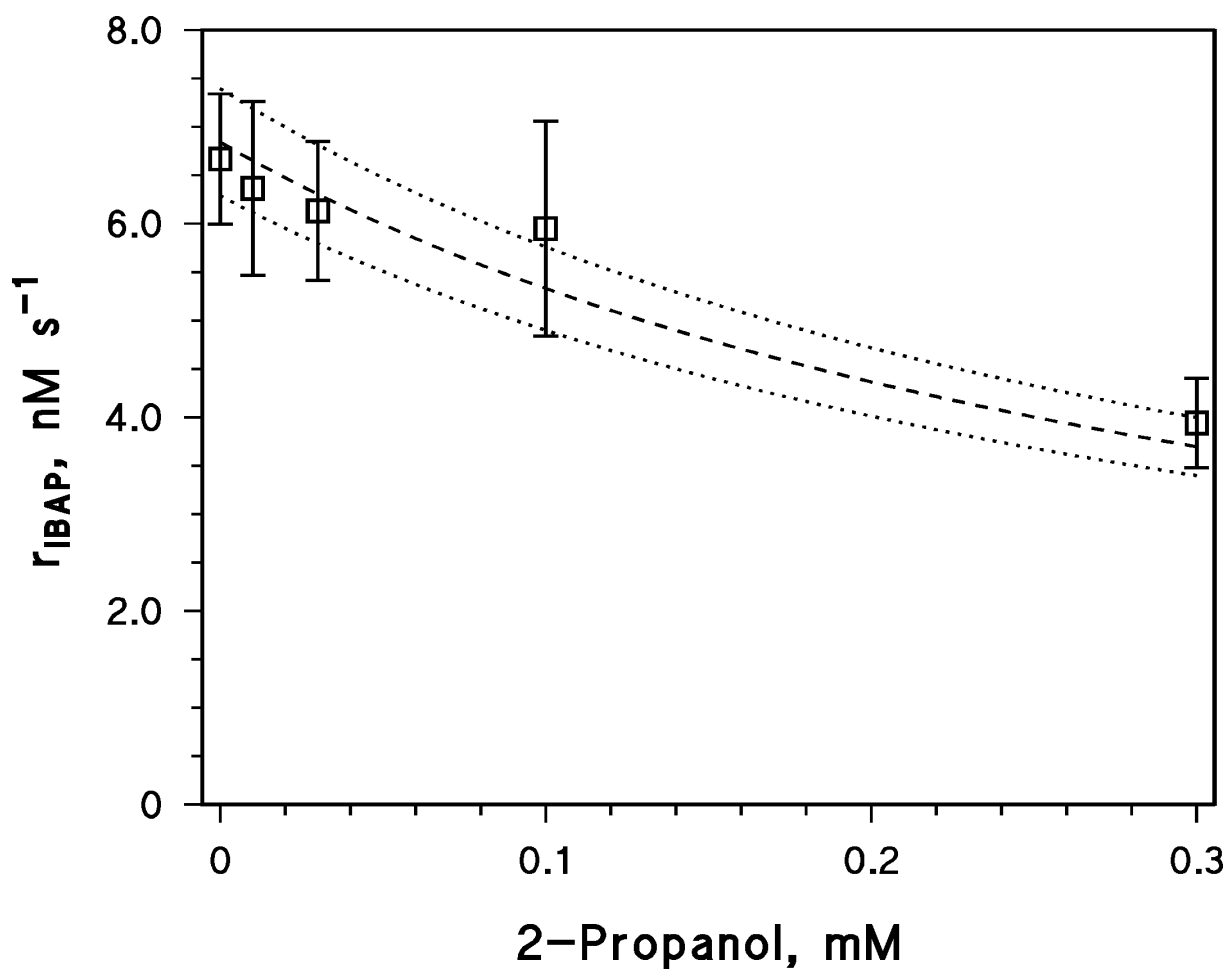
Figure 3. Initial transformation rates of 20 μM IBAP upon UVB irradiation of 1 mM H_2O_2, as a function of the concentration of added 2-propanol (pH 7). The dashed curve is the fit function (equation 5), the dotted ones represent the 95% confidence limits of the fit. Higher alcohol concentration values were not used to avoid interference with H_2O_2 photolysis (Nissenson et al., 2010).
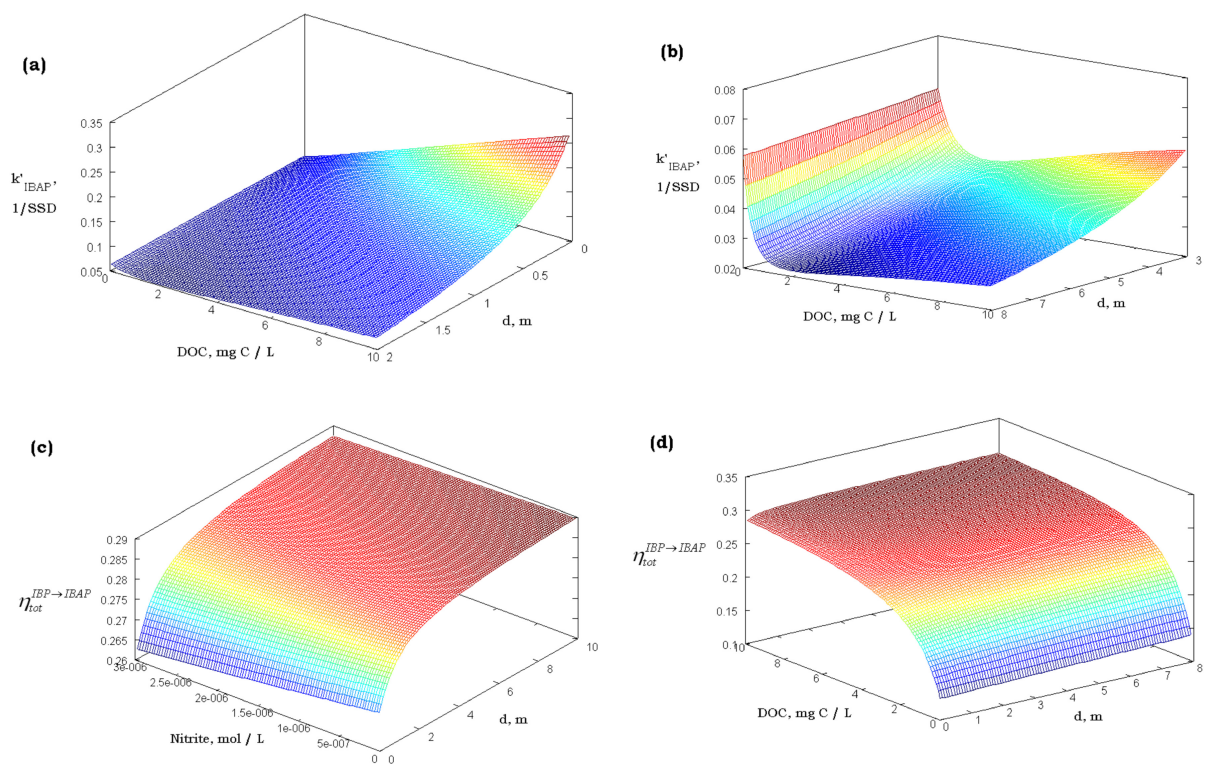
Figure 4. **(a,b)** Modelled first-order rate constant of IBAP photochemical formation (k'_{IBAP}), as a function of DOC and water depth d, in the ranges of 0-2 m **(a)** and 3-8 m **(b)**. Note that SSD = Summer Sunny Day equivalent to fair-weather 15 July at 45°N latitude. **(c,d)** Overall photochemical formation yield of IBAP from IBP ($\eta_{tot}^{IBP \rightarrow IBAP}$), as a function of nitrite and d **(c)** and of DOC and d **(d)**.

The following water parameters were kept constant (when applicable): nitrate 0.1 mM; nitrite 1 µM; DOC 5 mg C L^{-1}; carbonate 10 µM; bicarbonate 2 mM.
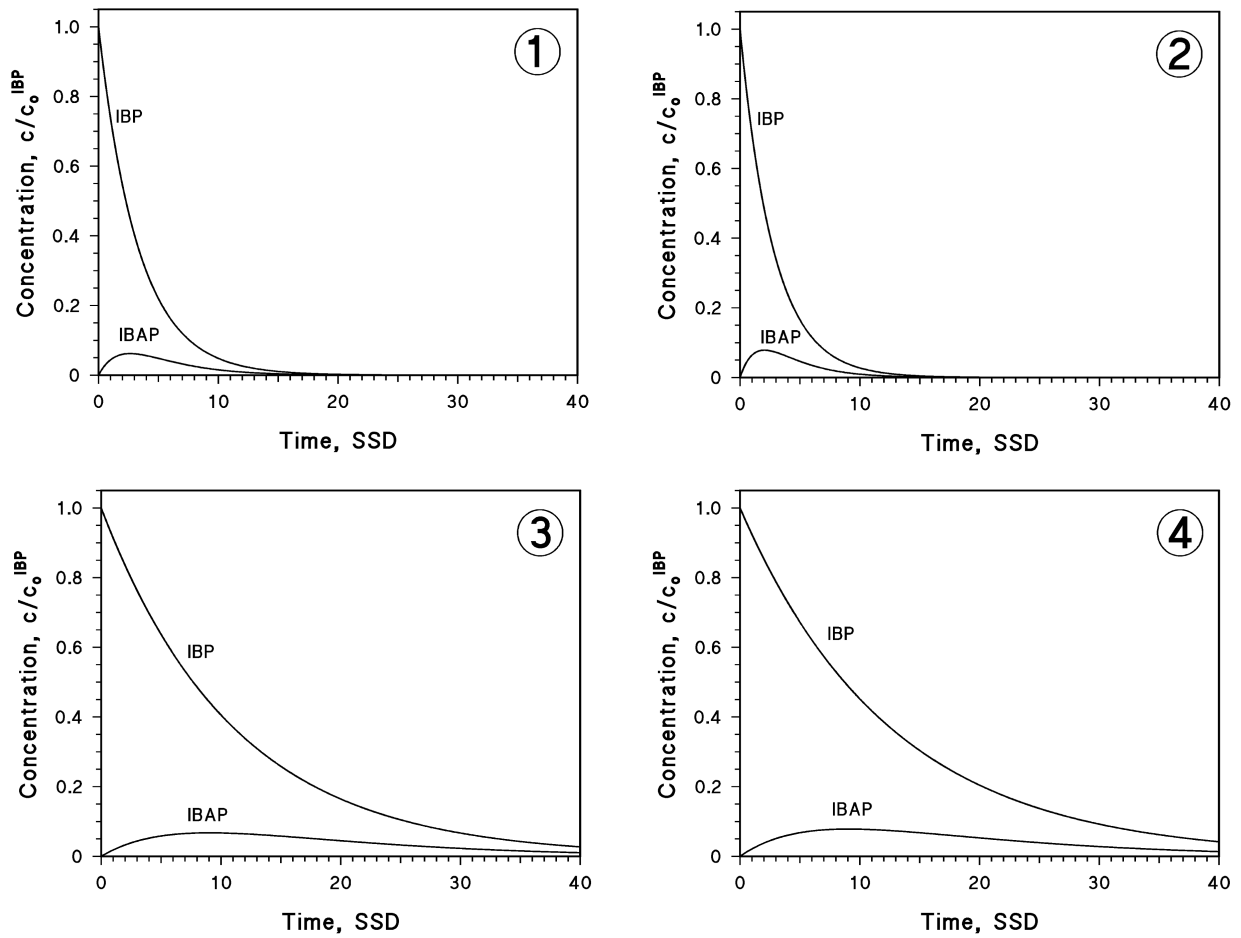
Figure 5. Modelled time trends of IBP and IBAP because of photochemical processes, under the following conditions: ① d = 1 m and DOC = 1 mg C L^{-1}; ② d = 1 m and DOC = 10 mg C L^{-1}; ③ d = 10 m and DOC = 1 mg C L^{-1}; ④ d = 10 m and DOC = 10 mg C L^{-1}. Other conditions, common to all four cases and less important for the trends, were as follows: 0.1 mM nitrate, 1 μM nitrite, 10 μM carbonate, and 2 mM bicarbonate.